The magnetic structures of some $Fe_{100-x}Zr_x$ metallic glasses

2003 J. Phys.: Condens. Matter 15 675

(http://iopscience.iop.org/0953-8984/15/4/308)

INSTITUTE OF PHYSICS PUBLISHING JOURNAL OF PHYSICS: CONDENSED MATTER

J. Phys.: Condens. Matter **15** (2003) 675–691 PII: S0953-8984(03)52792-8

The magnetic structures of some $Fe_{100-x}Zr_x$ metallic glasses

A R Wildes[1], J R Stewart[1], N Cowlam[2], S Al-Heniti[2], L F Kiss[3] and T Kemény[3]

[1] Institut Laue-Langevin, BP 156, 38042 Grenoble Cédex 9, France
[2] Department of Physics, University of Sheffield, Sheffield S3 7RH, UK
[3] Research Institute for Solid State Physics, H-1525, Budapest, POB 49, Hungary

Received 28 August 2002, in final form 5 December 2002
Published 20 January 2003
Online at stacks.iop.org/JPhysCM/15/675

Abstract

The spin-flip cross-sections of two samples each of $Fe_{90}Zr_{10}$ and $Fe_{92}Zr_8$ produced in two different laboratories were measured using the polarized neutron spectrometers IN20 and D7 at the Institut Laue-Langevin, Grenoble. All the samples have non-zero spin-flip cross-sections, with peaks at $Q \sim 3.1$ Å^{-1}, coinciding with the first maximum in the structure factor $S(Q)$, on a diffuse Q-dependent 'background'. The features change little on cooling to 2 K and persist above the Curie temperature. The samples are therefore all non-collinear ferromagnets, with significant ferromagnetic correlations between the non-collinear components of the moments. The compositions of the samples were shown to be correct to $\leqslant 0.1$ at.% by magnetic susceptibility measurements. The 'background' was found to be significantly larger in the spin-flip cross-sections of one set of the samples. Careful examination of neutron diffraction data measured using the LAD diffractometer, Rutherford Appleton Laboratory, showed that these samples had barely detectable impurities of α-Fe. The critical re-evaluation of previous data is therefore necessary as experimental results are evidently influenced by very low levels of crystalline impurities that are difficult to detect.

1. Introduction

The metallic glass system $Fe_{100-x}Zr_x$, $7 \leqslant x \leqslant 12$, is frequently used as a model system for the study of the effects of frustration on magnetic order. The spin Hamiltonian is believed to be Heisenberg-like; however, anisotropy and frustration result in the system having ferromagnetic and re-entrant spin-glass-like behaviour. This system has been extensively investigated experimentally and has inspired sophisticated band structure calculations [1, 2]. In spite of the volume of research undertaken so far, however, the magnetic structures of this system are still the subject of debate.

It is widely agreed that, with the exception of that with $x = 7$, each composition has two magnetic transition temperatures. On cooling, the samples undergo a phase transition from a paramagnetic to a ferromagnetic state at the Curie temperature T_C. On further cooling the samples undergo a second transition to a 'spin-frozen' state at temperature T_f, sometimes called T_{xy}. T_C decreases and T_f increases with increasing iron concentration until they meet at $x = 7$, where the sample transforms directly from a paramagnet to a spin glass at temperature T_{SG}. The magnetic phase diagram has been established using Mössbauer spectroscopy, magnetic susceptibility [3–5] and muon spin relaxation [6] techniques.

Early models constrained the magnetic moments to be collinear, the moments on the iron atoms varying in magnitude with some being antiferromagnetically oriented [7, 8]. The magnetic behaviour was thus attributed to changes in the sign of the exchange interaction due to local variations in the composition of the samples. The data from Mössbauer spectroscopy [4, 5, 9] unambiguously show that a large percentage of the magnetic moments can be *non*-collinear. This state was shown to be stable by band theory calculations [1]. Subsequent models have included non-collinear components in their description of the magnetic moments.

The exact nature of this non-collinear magnetism is the root of the debate concerning the magnetic structure. One group [10, 11] has suggested, on the basis of bulk magnetization and susceptibility data, that the magnetic structure is composed of ferromagnetic clusters whose magnetization directions are canted with respect to the mean ferromagnetic direction. These clusters are embedded in a ferromagnetic matrix, but isolated from it by zones of frustrated moments. A similar model, derived from the interpretation of magnetization data using a classical theory for the behaviour of superparamagnetic particles, suggests that clusters occupy the whole volume of the sample [12]. In both these cases, the interaction between clusters, the scaling of their size as a function of temperature, and the freezing of the dynamics between clusters at T_f are used to explain the observed temperature behaviour. There is evidence for clusters from neutron small-angle scattering [13, 14], the results of which suggest that, even for the temperatures $T_f \leqslant T \leqslant T_C$, the systems do not have conventional long-range ferromagnetic order.

The existence of clusters is strongly contested by Ryan *et al* [4–6, 15], who have examined the FeZr system with, among other techniques, magnetic susceptibility, Mössbauer spectroscopy [4, 5], neutron depolarization [15] and muon spin relaxation [6, 16]. They propose that an upper limit of only 0.5% of the iron atoms are present in clusters, and that, for $T < T_C$, the system is collinear ferromagnetic with very strong spin fluctuations. At T_f the fluctuations freeze, resulting in a non-collinear ferromagnetic structure with random disorder in the plane perpendicular to the mean moment direction, sometimes called asperomagnetism.

Reverse Monte Carlo (RMC) analysis of the structure factor, $S(Q)$, measured by means of unpolarized neutrons and x-rays has been used to derive a mean magnetic structure of a $Fe_{91}Zr_9$ metallic glass [17]. The $S(Q)$ were measured at a series of temperatures. The results of the RMC analysis could not rule out clusters, but suggested that an asperomagnetic structure was present for all $T < T_C$. The moments were non-collinear with a distribution peaked in the mean ferromagnetic direction and with an average angle to that direction of $\geqslant 53°$ at all temperatures. The authors were further able in their analysis to find the local environment in regions of extreme non-collinearity and have presented a phase diagram based on local coordination and the development of networks in the glass as a function of iron concentration.

It is important therefore not only to detect non-collinear magnetism in FeZr metallic glasses, but also to measure any *spatial correlation* between non-collinear components. Correlated non-collinearity would show that the system is not purely asperomagnetic, and could provide evidence for clusters or, alternatively, a 'wandering axis' [4] ferromagnet, whereby the moments are ferromagnetically correlated but the local ferromagnetic axis changes through

the sample. The best technique for this kind of study is neutron scattering with polarization analysis [18], since it can separate the scattering due to nuclear and collinear ferromagnetic structures from that due to non-collinear magnetism. In addition, as the cross-sections are directly proportional to the partial structure factors, it can be used to resolve any structure between the non-collinear components on an arbitrary length scale. It has been used with success to establish the presence (and absence) of non-collinear ferromagnetism in iron-based metalloid glasses [19, 20], and has shown in these systems that, where non-collinear ferromagnetism was found, an asperomagnetic structure was the most appropriate.

This paper presents the findings of neutron scattering measurements with polarization analysis on samples of $Fe_{90}Zr_{10}$ and $Fe_{92}Zr_8$. The samples have been measured at a selection of temperatures to determine the presence and nature of any non-collinear order in the various magnetic 'phases'. Samples of the same composition coming from different laboratories have been measured to test the consistency of results as a function of the sample 'batch'. Careful categorization of the samples is also therefore presented using magnetization and unpolarized neutron scattering. The data from neutron polarization analysis experiments are often subject to sample- or instrument-dependent depolarization, particularly in measurements of metallic glasses where the non-spin-flip signal is an order of magnitude larger than the spin-flip signal. To verify that the results were not artefacts of depolarization, the samples measurements were made on two different instruments, each with a different wavelength and instrument polarization efficiency. The neutron cross-sections have been presented in absolute units. A full account of the data analysis, with justified reasons for believing that the data have been correctly analysed and reduced, is given in the appendix. This work combines and expands on preliminary results presented previously [21, 22].

2. Experimental methods

2.1. Sample preparation

Samples of the metallic glasses $Fe_{92}Zr_8$ and $Fe_{90}Zr_{10}$ were prepared at both the University of Sheffield and at the Research Institute for Solid State Physics, Budapest. Parent ingots were prepared with negligible weight loss from spectroscopically pure elements. The Sheffield ingots were made by argon-arc melting while the Budapest ingots were forged in a cold crucible. The metallic glass ribbons were produced by conventional chill-block melt spinning. The Sheffield melt-spin apparatus used a steel wheel with a rim speed of approximately 50 m s^{-1}. The Budapest apparatus had a low-alloyed high-strength and high-thermal-conductivity copper wheel with a rim speed of approximately 35 m s^{-1}. The Sheffield samples were spun in a helium atmosphere while the Budapest samples were spun in hydrogen. All samples were ribbons $\approx$25 μm thick and $\approx$1 mm wide; however, the appearance of the samples differed—the Budapest samples were smooth and homogeneous while the Sheffield samples were somewhat striated and less regular. There was no evidence of hydrogen uptake in the Budapest samples [22].

2.2. Magnetic susceptibility

Examination of the magnetic phase diagram shows that the critical temperatures for this system change dramatically with composition [3, 6]. Consequently, magnetic susceptibility measurements have been carried out to confirm the composition of the samples. The susceptibility measurements were made on a Quantum Design SQUID magnetometer, type MPMS-5S, at the Research Institute for Solid State Physics, Budapest. Short lengths

of ribbon (∼4 mm) were cut from different parts of each of the four samples for these measurements. Each piece was mounted on a silicon plate with silicon grease. The samples were cooled to 5 K in zero field. A field of 10 Oe was then applied to the sample. The field was maintained for the measurements.

2.3. Unpolarized neutron scattering

X-ray diffraction would normally be used to quantify the glassy nature of the samples; however, due to fluorescence from the zirconium atoms with Mo Kα radiation, the results using this technique proved to be very difficult to analyse [23]. Neutron diffraction techniques were therefore used. The measurements of the ribbons were made at room temperature on the LAD diffractometer at the ISIS neutron facility, Rutherford Appleton Laboratory, UK. The ribbons were wound onto frames of brass and stainless steel as described previously [19, 20]. The measurements were carried out under vacuum to reduce air scattering. No magnetic field was applied to the samples during the measurements. Background and vanadium measurements were also made to ensure correct data analysis and normalization. The LAD instrument had seven paired banks of detectors, arranged symmetrically around the sample at angles of 5°, 10°, 20°, 35°, 60°, 90° and 150°. Each detector bank covered a different range in Q and had a different resolution. The data collected in different banks were normalized and subsequently combined using the ATLAS set of programs [24].

The resulting data are the unpolarized neutron cross-sections. Assuming that the magnetic contribution to the cross-sections at 300 K is very small relative to the nuclear contribution, the general expression for the cross-section,

$$\frac{\mathrm{d}\sigma}{\mathrm{d}\Omega} = \left|\left\langle \sum_l b_l \exp(\mathrm{i}\boldsymbol{Q}\cdot\boldsymbol{R}_l)\right\rangle\right|^2,$$

where b_l is the scattering length of the lth atom at a position $\boldsymbol{R}_l$, can be written for these $Fe_{100-x}Zr_x$ glasses as

$$\frac{\mathrm{d}\sigma}{\mathrm{d}\Omega} = \frac{N}{4\pi}\{\langle b\rangle^2 S(Q) + (\langle b^2\rangle - \langle b\rangle^2) + \sigma_{inc}\} \tag{1}$$

where

$$\langle b\rangle = (1 - x/100)b_{\mathrm{Fe}} + (x/100)b_{\mathrm{Zr}},$$
$$\langle b^2\rangle = (1 - x/100)b_{\mathrm{Fe}}^2 + (x/100)b_{\mathrm{Zr}}^2.$$

Here b_{Fe} and b_{Zr} are the bound coherent scattering lengths and σ_{inc} the total incoherent cross-section, which are all tabulated [25]. The second term in equation (1) is equivalent to the Laue monotonic scattering with x-rays and for these binary alloys may be written as

$$\langle b^2\rangle - \langle b\rangle^2 = (x/100)(1 - x/100)(b_{\mathrm{Fe}} - b_{\mathrm{Zr}})^2.$$

The structure factor, $S(Q) = \frac{1}{N}\sum_{l,l';l\neq l'}\langle\exp(\mathrm{i}\boldsymbol{Q}\cdot(\boldsymbol{R}_l - \boldsymbol{R}_{l'}))\rangle$, can therefore be obtained from the normalized mean coherent cross-section by subtracting the calculated contributions:

$$\frac{N}{4\pi}\{(x/100)(1 - x/100)(b_{\mathrm{Fe}} - b_{\mathrm{Zr}})^2 + \sigma_{inc}\},$$

and, if required, the reduced radial distribution function, $G(r)$, can then be derived from $S(Q)$ by Fourier transformation:

$$G(r) = 4\pi r(\rho(r) - \rho_0) = \frac{2}{\pi}\int_0^\infty Q(S(Q) - 1)\sin Qr\,\mathrm{d}Q.$$

Here, ρ_0 is the average atomic number density and the radial distribution function is given by $\mathrm{RDF} = 4\pi r^2\rho(r)$.

2.4. Polarized neutron scattering

Several polarized neutron scattering measurements were made on the samples using spectrometers at the Institut Laue-Langevin, Grenoble. The majority of the experiments were carried out on the IN20 three-axis spectrometer. Further measurements, as confirmation of the IN20 results, were carried out on the D7 diffuse scattering spectrometer.

A ferromagnetic sample must be single domain for a neutron polarization analysis experiment; otherwise it will depolarize the beam. A magnetic field was therefore applied to the samples for all the measurements with the aid of a superconducting cryomagnet. The cryomagnet was capable of cooling the sample below 2 K with an accuracy of better than ± 0.1 K and establishing homogeneous fields over the sample to $< \pm 1\%$. A vertical saturating field of 20 kOe was chosen for all of the measurements. This field has been shown to saturate the domains in these samples and is consistent with previous measurements on other metallic glass systems [19, 20]. The field direction determined the direction of the guide field at the sample position and therefore the neutron polarization axis $\hat{\boldsymbol{P}}$. The ribbon samples were wound onto frames similar to those used for the LAD measurements, with the ribbons aligned such that the long axis of the ribbons was always parallel to the field direction.

The application of a magnetic field is known to influence any possible non-collinearity in the $Fe_{100-x}Zr_x$ system, indeed $Fe_{90}Zr_{10}$ is believed to be collinear at 4.2 K in a field of 21 kOe [9]. $Fe_{92}Zr_8$, however, is quoted as being non-collinear in fields up to 50 kOe, with the moments making an average angle of $\sim 30^\circ$ to the mean ferromagnetic direction [9]. Considerable scattering from non-collinear order was therefore expected for at least one of the samples with the given applied field.

The IN20 spectrometer was configured with a polarizing Heusler monochromator and analyser, with the incident and final wavevectors fixed at $k_i = k_f = 4.1$ Å^{-1}. Higher-order (unpolarized) contamination was removed with a graphite filter. The horizontal divergence of the instrument from reactor to detector was limited with the aid of Soller collimators to open–60′–60′–120′. The FWHM resolution of this configuration was $\Delta Q = 2.7 \times 10^{-2}$ Å^{-1} and $\Delta E = 3.0$ meV at $Q = 3.1$ Å^{-1}. The four polarization-dependent neutron cross-sections were measured with the aid of precession coil spin flippers in the incident and scattered beams. Tuning of the flippers by scattering from silicon resulted in optimum flipping ratios of ~ 18. The scattering was measured on IN20 for a range of momentum transfers of $1 \leqslant Q \leqslant 6.3$ Å^{-1}. IN20 has a single detector, and the sample was rotated with the detector such that the sample always bisected the angle between the incident and scattered beams.

The D7 spectrometer was configured with a graphite monochromator and an incident wavevector $k_i = 2.027$ Å^{-1}. The neutron beam was polarized and analysed with supermirror benders in the incident and scattered beams, and the incident neutron spin state was determined with a precession coil spin flipper. The optimum flipping ratio was ~ 40. No flipper was used in the scattered beam, and therefore only two of the four polarization-dependent cross-sections could be measured. The FWHM resolution of the instrument was $\Delta Q = 0.15$ Å^{-1} and $\Delta E = 18.0$ meV at $Q = 3.1$ Å^{-1}. A vertical cryomagnet was used for the D7 measurements; therefore the neutron polarization was always perpendicular to the scattering vector. The instrument had 32 detectors and could thus simultaneously measure a range of momentum transfer $0.35 \leqslant Q \leqslant 4$ Å^{-1}, although due to shielding by the sample frame no accurate data could be collected for $1 \leqslant Q \leqslant 2.2$ Å^{-1}. Further measurements to smaller Q are planned, and therefore only the data for $2.3 \leqslant Q \leqslant 4$ Å^{-1} will be presented in this paper. The detectors were not moved and the sample orientation stayed fixed for all the measurements.

While both non-spin-flip and spin-flip scattering were measured, only the spin-flip results will be presented. The spin-flip cross-sections are directly proportional to the correlation

Table 1. Summary of the transition temperatures for the samples of the same composition made in the two laboratories, as measured by a SQUID magnetometer in a field of 10 Oe.

	Curie temperature, T_C (K)	Freezing temperature, T_f (K)
$Fe_{90}Zr_{10}$ (Sheffield)	232 ± 2	10 ± 0.5
$Fe_{90}Zr_{10}$ (Budapest)	228 ± 1	12.8 ± 0.5
$Fe_{92}Zr_8$ (Sheffield)	180 ± 2	61 ± 2
$Fe_{92}Zr_8$ (Budapest)	173 ± 2	67 ± 2

function of the *non-collinear* components of the moments. Assuming that any non-collinear magnetism is isotropic in the plane perpendicular to the mean ferromagnetic direction, the coherent part of the spin-flip cross-sections, $\partial\sigma^{sf}/\partial\Omega$, may be written in SI units as

$$\frac{\partial\sigma^{sf}}{\partial\Omega} = \frac{1}{2}(1 + (\hat{\boldsymbol{P}} \cdot \hat{\boldsymbol{Q}})^2)\left|\left\langle \sum_l p_{\perp l}(Q) \exp(\mathrm{i}\boldsymbol{Q} \cdot \boldsymbol{R}_l)\right\rangle\right|^2$$
$$= \frac{1}{2}(1 + (\hat{\boldsymbol{P}} \cdot \hat{\boldsymbol{Q}})^2)\left(\frac{\gamma e^2}{m_e}\right)^2\left|\left\langle \sum_l f_l(Q)\mu_{\perp l} \exp(\mathrm{i}\boldsymbol{Q} \cdot \boldsymbol{R}_l)\right\rangle\right|^2 \quad (2)$$

where $p_{\perp l}$ is the non-collinear component of the magnetic scattering length of the lth atom, $f(Q)$ is the magnetic form factor [26] and $\mu_{\perp l}$ is the non-collinear projection of the lth magnetic moment in units of μ_B. $\hat{\boldsymbol{P}}$ and $\hat{\boldsymbol{Q}}$ are the unit vectors in the direction of the neutron polarization and the scattering vector respectively.

Comparison of equation (2) with (1) shows a similarity of form, with the magnetic scattering length, $p_{\perp l}$, replacing the nuclear scattering length, b_l. Equation (2) can therefore be expressed with a magnetic structure factor that will depend on how the non-collinear components of the magnetic moments are *spatially correlated*. Neutron scattering with polarization analysis is the only technique not only able to directly detect non-collinear magnetism, but also able to measure spatial correlations in a non-collinear magnetic structure. For example, an ideal asperomagnet has no correlations between the non-collinear moments and the non-collinear magnetic structure factor will be unity for all Q. The measured cross-sections would therefore be smoothly decreasing with increasing Q, modulated by the square of the form factor, $f^2(Q)$. Spatial correlation will give rise to a magnetic structure factor that varies with Q, and therefore peaks will be observed in the spin-flip cross-sections.

As in previous experiments [20], background and instrument calibration measurements were made to correct for instrument inefficiency and to calculate absolute cross-sections. A full account of the procedures used and justification of the derived cross-sections are given in the appendix.

3. Results

3.1. Atomic composition and quality of the samples

SQUID magnetometer measurements clearly show two transition temperatures, corresponding to T_C and T_f, for each of the samples. The summary of the measured transition temperatures is given in table 1. The transition temperatures for samples of the same composition correspond closely with one another, and closely with the expected T_C and T_f for the desired compositions. The compositions of the samples are therefore accurate to $\leqslant 0.1$ at.%.

Examination of the measured $S(Q)$ for the samples also clearly confirms their glassy nature. Figure 1 shows the $S(Q)$ for each of the four samples, derived from the normalized

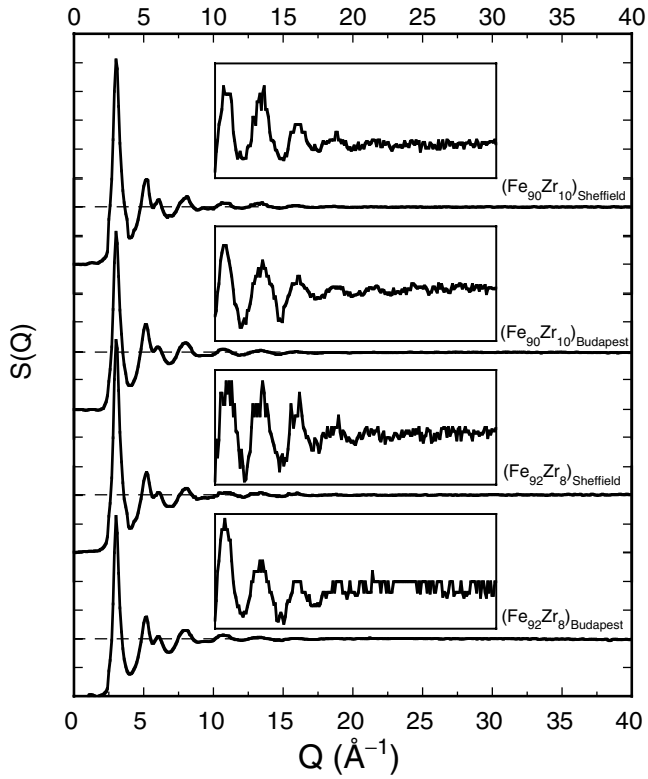

Figure 1. The structure factors $S(Q)$ for the four $Fe_{100-x}Zr_x$ samples, as derived from the combined data from all the LAD detector banks. The data for the range $10 \leqslant Q \leqslant 30$ Å^{-1} are shown for each on an expanded scale.

and combined data from all the detector banks on the LAD instrument. The data for the range $10 \leqslant Q \leqslant 30$ Å^{-1} for each sample are also presented with an expanded vertical scale. Each $S(Q)$ shows seven or more maxima, proving that these samples are good examples of metallic glasses.

3.2. Polarized neutron measurements at 20 kOe as a function of temperature

Three temperatures of interest were chosen for the measurements: 300 K ($>T_C$ for all the samples); 135 K ($T_C > 135$ K $> T_f$); and 2 K ($<T_f$). Due to time restrictions, measurements were made at only a few of these temperatures for some of the samples on IN20, while measurements were made at all the temperatures on D7. The magnetic behaviour of the samples was expected to have a field history dependence due to the presence of the 'frozen' phase, and consequently two sets of measurements were carried out at 135 and 2 K on IN20: cooling from 300 K in zero field and cooling from 300 K in 20 kOe. The application of a field on cooling had no measurable effect on the observed scattering, and consequently the IN20 data at each temperature were combined to improve statistics. All the samples were cooled from 300 K in a field of 20 kOe for the D7 measurements. The results for all the measured spin-flip cross-sections are summarized in figures 2 and 3. There is excellent correspondence between the derived spin-flip cross-sections measured independently on the two different instruments, confirming that the measurements and resultant analysis have been correctly performed.

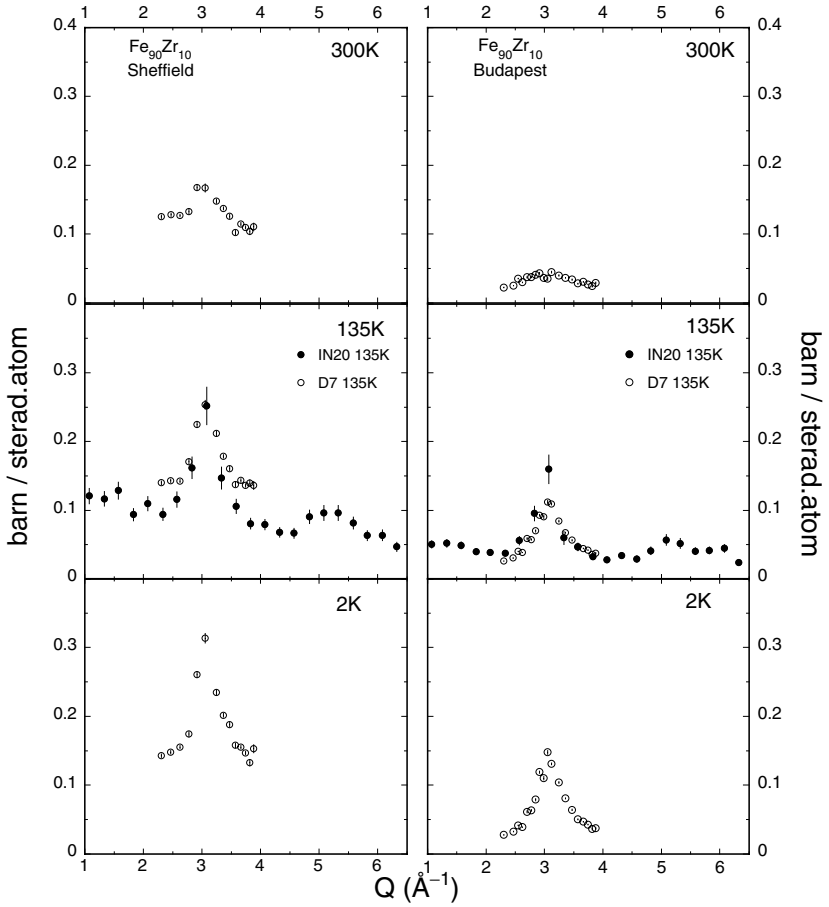

Figure 2. The measured spin-flip cross-sections for $Fe_{90}Zr_{10}$ at 20 kOe as a function of temperature.

All the samples at all temperatures have a non-zero spin-flip cross-section, and therefore they all have some degree of non-collinear ferromagnetism. The energy integration of the measurements, in particular for those of the IN20 spectrometer, is small; therefore the cross-sections result from quasi-static moment orientations. Two features are immediately evident in the cross-sections. Firstly, all the measured spin-flip cross-sections have a peak at $Q \sim 3.1$ Å^{-1}, corresponding to the first maximum in $S(Q)$. The second feature is the appearance of a very broad, diffuse component in the cross-sections that is considerably larger in the Sheffield samples than in the Budapest samples.

The diffuse component, and its dependence on the sample, has been noted in previous publications detailing the preliminary estimations of the spin-flip cross-sections of $Fe_{90}Zr_{10}$, as measured on IN20 [21, 22]. The data presented did not show any peaks. This was due to incorrect adjustment of the data for polarization inefficiencies. The flipping ratios used to correct the data were measured using the main beam of IN20. For reasons related to increased non-polarized background at very small angles and beam size inconsistencies, these values were smaller than the real flipping ratios for the measurement ($\sim$13 for the main beam versus $\sim$18 for the measurement). Using smaller flipping ratios results in an *over*correction for polarization inefficiency, which removed the peaks in the previously presented data and has, on close inspec-

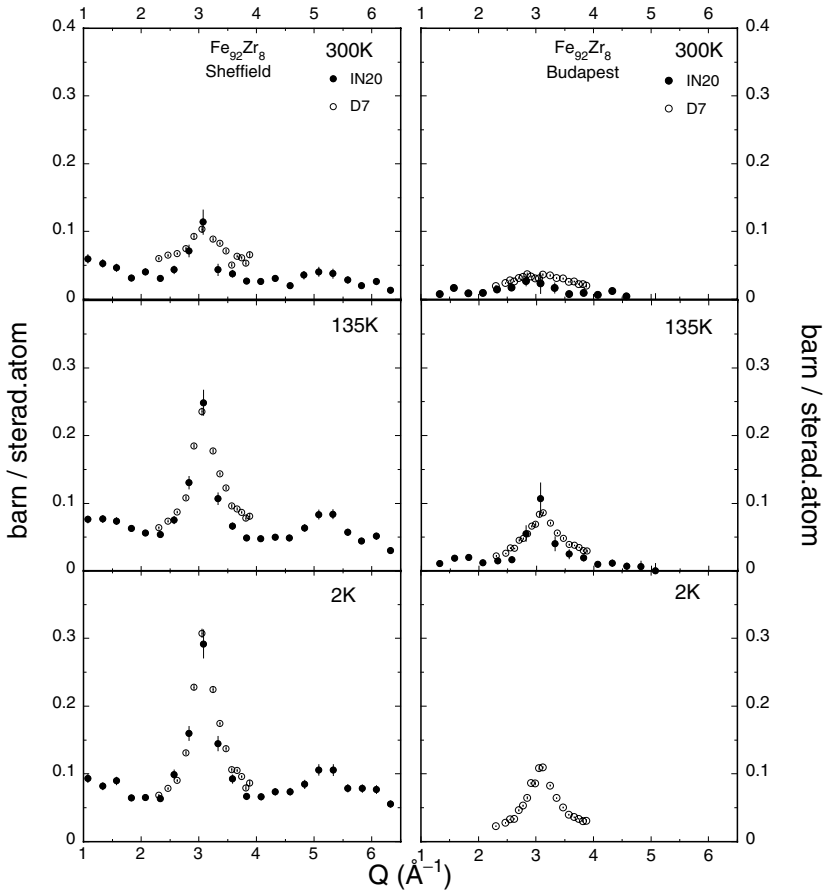

Figure 3. The measured spin-flip cross-sections for $Fe_{92}Zr_8$ at 20 kOe as a function of temperature.

tion, resulted in a slight *negative* peak for the Budapest $Fe_{90}Zr_{10}$ sample. It is believed that the polarization inefficiency has now been correctly accounted for, as is apparent by the excellent correspondence between the IN20 data and the independently measured and analysed D7 data.

The IN20 and D7 results give equivalent sizes and widths of the peaks at $Q \sim 3.1$ Å^{-1} for $T < T_C$, even though the energy window differs by a factor of six. The peaks are therefore due to a static non-collinear ferromagnetic structure, in contradiction to proposals that FeZr glasses are collinear ferromagnets with strong spin fluctuations for $T_f < T < T_C$ [6]. The peaks suggest that the non-collinear components are ferromagnetically correlated over many atoms. Such spatial correlation may be present in a cluster [11, 12] or a 'wandering axis' ferromagnet [4]. The widths of the peaks at 2 K are comparable to the corresponding widths of the equivalent peaks in $S(Q)$, suggesting that the non-collinear magnetic coherence length is of the same order as the structural coherence length, $\Delta Q \sim 0.63$ Å^{-1} or $\xi = 2\pi/\Delta Q \sim 10$ Å. The magnitudes of the peaks at 2 K are comparable for all samples. Increasing the temperature to 135 K has little effect on the spin-flip cross-sections of any of the samples. The peaks at $Q \sim 3.1$ Å^{-1} are slightly smaller in magnitude but are similar in width.

As would be expected, raising the temperature to $T > T_C$ has a dramatic effect on the spin-flip cross-sections. The data at 300 K still show a weak peak at $Q \sim 3.1$ Å^{-1}, although the width of the peak is now much broader. The magnitudes of the cross-sections as measured

on D7, which integrated the scattering over an energy range of ∼18 meV, are marginally larger than those measured on IN20, which are integrated over ∼3 meV, as would be expected in the presence of strong magnetic fluctuations. Non-collinear ferromagnetism, correlated over shorter length scales and with an energy width within the window of the instruments, clearly persists above the Curie temperature. This is in agreement with previous Mössbauer studies of these metallic glasses [9], although the collinear state for the $Fe_{90}Zr_{10}$ composition is believed to be achieved at 21 kOe, putting it at the limit of this measurement. Similar ferromagnetic short-range order is observed well above T_C in other iron compounds, including Invar and anti-Invar alloys [27].

4. Discussion

Before discussing the details of the experimental data, it should be re-stated that all the measurements were made in a field of 20 kOe and consequently the conclusions relate to the structure at that field. Indeed, previous measurements with Mössbauer spectroscopy indicate that the application of a field reduces non-collinearity in this system [9].

4.1. The source of the sample dependence of $\partial\sigma^{sf}/\partial\Omega$

The diffuse component of the spin-flip cross-sections, clearly seen in the Sheffield samples but much reduced in the Budapest samples, can be attributed to a magnetic structure that is stimulated by a very small amount of crystalline α-Fe present as an impurity. The presence of this contamination has previously been alluded to in magnetization measurements [21]. Conclusive proof of the existence of such a phase is revealed by close and careful examination of the unpolarized neutron scattering data from LAD.

Figure 1 shows that all four of the FeZr samples have structure factors $S(Q)$ indicative of a genuine glassy structure [23]. Careful examination of $S(Q)$ does reveal some differences between samples, particularly in the height of the first peak. It was first thought that the differences were the result of states of structural relaxation [22]. The $S(Q)$ in figure 1, derived from the data combined from all the LAD detector banks, fail to provide a consistent picture of the possible structural differences between the various samples. This suggested that the differences were being masked in the combination process by subtle variations in the absorption paths of the neutrons and by instrumental resolution for the different detector banks. The comparison was therefore restricted to the 150° detector bank, which had an excellent resolution of $\Delta Q/Q = 0.5\%$ and has provided the most stringent tests of glassy and amorphous structures in the past [28].

Figures 4 and 5 show the $S(Q)$ taken from the 150° detector bank. Small Bragg-like features are clearly visible, particularly for the Sheffield samples although traces of the features are also present in the $Fe_{92}Zr_8$ Budapest $S(Q)$. The Bragg-like features become prominent when the difference in $S(Q)$ is taken between Sheffield and Budapest samples. The difference plots are also shown in figures 4 and 5. The sharp peaks in the plots can be indexed on the bcc α-Fe structure, with the calculated Bragg peak positions marked in the figure. Aside from the peaks, there is essentially no difference in $S(Q)$ between the Sheffield and Budapest samples, indicating that the volume per cent that is glass-like is in the same state of structural relaxation in all the samples. The only difference between the structures of the samples from the different laboratories is therefore due to a very small, barely measurable crystalline iron impurity that is nevertheless larger in the Sheffield samples than the Budapest samples.

The volume fraction of the sample that has the α-Fe impurity can be estimated from the magnetization measurements. In total, three short lengths of each sample were measured in the

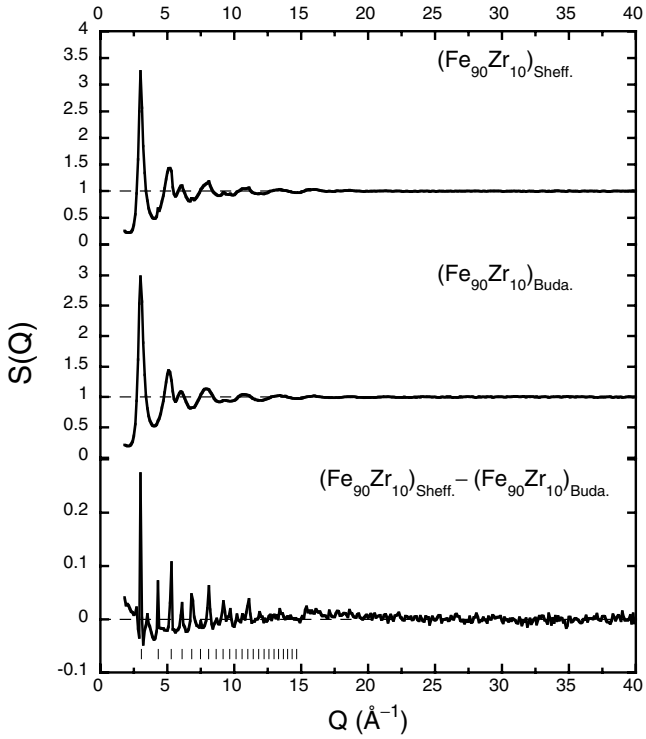

Figure 4. The structure factors $S(Q)$ for $Fe_{90}Zr_{10}$, as measured with the 150° detector bank on LAD. Also shown is the difference between the two $S(Q)$, with the Bragg positions for α-Fe marked below.

SQUID magnetometer. Of the 12 lengths, one of the Sheffield-made $Fe_{90}Zr_{10}$ lengths showed an unambiguous magnetization above the Curie temperature, corresponding to $\sim$0.5 vol% α-Fe content [21]. The other pieces of this sample also showed some, considerably smaller, traces of magnetism above T_C. The Sheffield $Fe_{92}Zr_8$ lengths also registered very small traces of α-Fe, with the maximum observable magnetization being equivalent to 0.2 vol% bcc-Fe for one of the lengths. No trace of any crystalline impurity could be measured within the sensitivity of the SQUID magnetometer for any of the Budapest samples, putting an upper limit of 0.05 vol% bcc-Fe for these samples.

A degree of heterogeneity is an inevitable consequence of any non-equilibrium processing technique, such as quenching techniques. It is one of the surprising properties of these samples that a low crystalline fraction undetected by the usual techniques influences magnetic collinearity to such a marked degree. A small volume percentage of crystalline impurities in a glassy matrix is expected to produce a high degree of stress in a sample. The stress is obviously heterogeneous, depending on local structure and inhomogeneity, and will invariably influence the magnetic structure through magnetostriction and local anisotropy. The effect is difficult to quantify, particularly when the crystalline iron is barely detectable by all but the most stringent of tests, and future experiments will explore the connection further.

The presence of trace impurities of crystalline iron may also help explain the diversity in the models for the magnetic structure of $Fe_{100-x}Zr_x$. A tiny crystalline impurity will introduce a sample dependence, meaning that measurements on samples from different laboratories using different techniques may not be directly comparable. Interestingly, the diffuse cross-

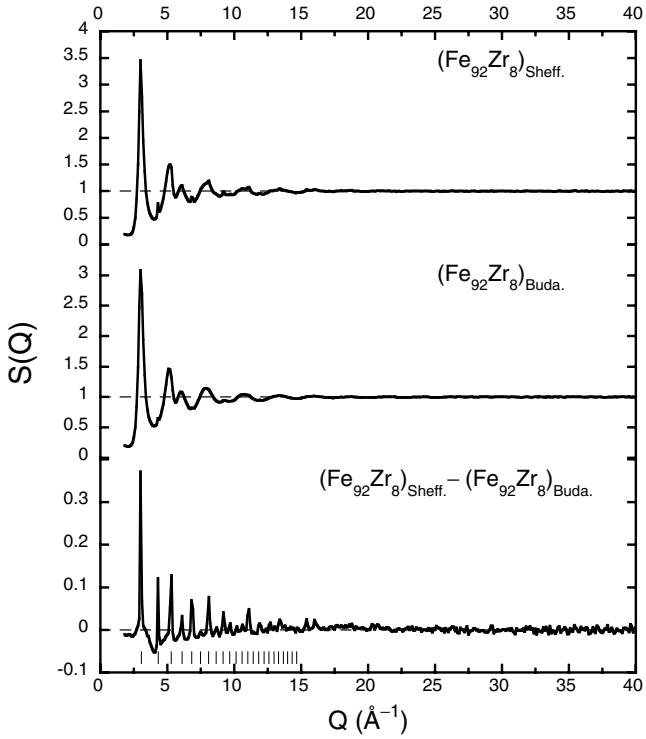

Figure 5. The structure factors $S(Q)$ for $Fe_{92}Zr_8$, as measured with the 150° detector bank on LAD. Also shown is the difference between the two S(Q), with the Bragg positions for α-Fe marked below.

sections as measured on D7, with its larger energy integration, may be slightly larger than those measured on IN20, particularly for the Sheffield $Fe_{90}Zr_{10}$ sample. It is possible that the crystalline impurity also influences any magnetic fluctuations. It is therefore not established whether subsequently derived models for the magnetic structure are universal or are specific to the measured sample.

Previous experiments on similar metallic glasses [19, 20] have shown diffuse spin-flip cross-sections that decrease in magnitude with increasing Q in a form-factor-like manner. Such behaviour is consistent with a magnetic structure that has little or no correlation between the non-collinear components of the moments, such as in an asperomagnet. The Sheffield samples have a significant diffuse component in their spin-flip cross-sections, which is much reduced in the Budapest samples. The Sheffield samples have the greater percentage of crystalline iron contamination, and therefore it may be concluded that the presence of a trace impurity of α-Fe will induce a random, asperomagnet-like structure.

4.2. The magnetic structures of the four samples

As indicated by equation (2), the data may be further analysed to quantify the structure. Ideally a sophisticated analysis would be applied, extracting non-collinear radial distribution functions, ascertaining coherence lengths and attempting to determine the ensemble-averaged orientation of the moments. It is, unfortunately, impossible to determine these properties unambiguously and quantitatively when the data have only been measured over a limited range of Q. The data can be analysed semi-quantitatively, however, using a few simple approximations.

Table 2. Summary of the resulting parameters from fitting a Gaussian function on a sloping background to the IN20 data ($Q \leqslant 4.5$ Å^{-1}) for the samples at 135 K, with the calculated magnitudes of the non-collinear moments contributing to the correlated and non-correlated order.

	Background intercept at $Q = 0$ (b sr^{-1}/ atom)	Gradient on the sloping background (b sr^{-1} Q^{-1}/ atom)	Amplitude of Gaussian	σ for Gaussian	$\langle\mu_\perp^2\rangle^{1/2}$ for $\partial\sigma^{sf}_{diff}/\partial\Omega$ (μ_B)	$\langle\mu_\perp^2\rangle^{1/2}$ for $\partial\sigma^{sf}_{corr}/\partial\Omega$ (μ_B)
Sheffield	0.135	−0.015	0.13	0.23	1.94	1.8
$Fe_{90}Zr_{10}$	±0.007	±0.002	±0.02	±0.03	±0.05	±0.1
Budapest	0.054	−0.005	0.10	0.22	1.25	1.5
$Fe_{90}Zr_{10}$	±0.004	±0.001	±0.02	±0.03	±0.05	±0.1
Sheffield	0.079	−0.007	0.18	0.18	1.48	2.0
$Fe_{92}Zr_8$	±0.005	±0.002	±0.03	±0.02	±0.05	±0.2
Budapest	0.019	−0.002	0.09	0.19	0.73	1.4
$Fe_{92}Zr_8$	±0.003	±0.001	±0.02	±0.03	±0.06	±0.2

As peaks and underlying diffuse, form-factor-like features are visible in the spin-flip cross-sections, it seems likely that the non-collinear magnetic structure consists of regions that are spatially correlated with additional randomly correlated non-collinear moments. Equation (2) can then be manipulated to have two terms that describe these parts:

$$\frac{\partial\sigma^{sf}}{\partial\Omega} = \frac{\partial\sigma^{sf}_{diff}}{\partial\Omega} + \frac{\partial\sigma^{sf}_{corr}}{\partial\Omega}. \tag{3}$$

$\partial\sigma^{sf}_{corr}/\partial\Omega$ is the part that expresses the spatial correlation, and may also be written as

$$\frac{\partial\sigma^{sf}_{corr}}{\partial\Omega} \propto \frac{1}{2}(1 + (\hat{\boldsymbol{P}}\cdot\hat{\boldsymbol{Q}})^2)\left(\frac{\gamma e^2}{m_e}\right)^2 f^2(Q)\langle\mu_\perp^2\rangle S_\perp(Q). \tag{4}$$

where $f(Q)$ is an appropriate magnetic form factor. The structure factor for the spatially correlated non-collinear moments, $S_\perp(Q)$, also accounts for strong small-angle scattering [13, 14] and possible scattering due to short-range magnetic order. The function $S_\perp(Q)$ is therefore separate from the atomic structure factor $S(Q)$ in equation (1).

The part of the cross-section due to randomly correlated moments, $\partial\sigma^{sf}_{diff}/\partial\Omega$, accounts for the broad 'background'. In previous publications, this part has been expressed as a broadened form factor [19–21, 29, 30]. The same equation could again be applied here; however, it is difficult to draw quantitative conclusions from any fitted parameters as short-range spatial correlation would interfere with the broadening parameter.

An extremely simple function of a Gaussian, for $\partial\sigma^{sf}_{corr}/\partial\Omega$, on a sloping background, for $\partial\sigma^{sf}_{diff}/\partial\Omega$, was therefore fitted to the data. Only the IN20 data at 135 K were fitted, making the restriction $Q \leqslant 4.5$ Å^{-1} to account for only the first peak at $Q \sim 3.1$ Å^{-1}. The amplitude of the Gaussian can then be used to give some quantitative measure of the volume fraction of the sample that has a correlated non-collinear structure, while the sloping background will give some measure of the volume fraction with a random non-collinear structure. The fit results are presented in table 2.

Also presented in table 2 are estimations for the magnitudes of $\langle\mu_\perp^2\rangle^{1/2}$ for the correlated and random non-collinear structures. The values of $\langle\mu_\perp^2\rangle^{1/2}$ for the random structure were estimated by taking the $Q = 0$ intercepts of the sloping background, where it is expected that $\partial\sigma^{sf}_{diff}/\partial\Omega = \frac{1}{2}(\gamma e^2/m_e)^2\langle\mu_\perp^2\rangle = 0.036\langle\mu_\perp^2\rangle$ b sr^{-1}/atom. The values are most probably

overestimates of the random moments, given that $\partial\sigma^{sf}_{diff}/\partial\Omega$ is also subject to a form factor and therefore the $Q = 0$ intercept will be smaller than the intercept of the fitted straight line.

In order to calculate the values of $\langle\mu^2_\perp\rangle^{1/2}$ for the correlated structure from equation (4), magnitudes of $f^2(Q)$ and $S_\perp(Q)$ had to be estimated. The values of $f^2(Q)$ were calculated using the analytic approximation for the normalized form factor [26] and, in keeping with previous work on iron-based metallic glasses [19, 20], the chosen form factor was that of Fe^{3+}. The magnitude of $S_\perp(Q)$ was estimated from the structure factors $S(Q)$ in figure 4. Inspection of the figure shows that the peaks at $S(Q = 3.1\ \text{Å}^{-1}) \sim 3$. As the peak in the spin-flip cross-sections is due to ferromagnetic correlations, it may be assumed that $S_\perp(Q = 3.1\ \text{Å}^{-1})$ has a similar value. Again, the values of $\langle\mu^2_\perp\rangle^{1/2}$ are likely to be overestimated as no accounting has been made for the broadening of the form factor by the glassy nature of the sample [29].

Despite the simplicity of the fitting function and the overestimation of the moments, some semi-quantitative conclusions may be drawn. The fitted parameters clearly confirm the observation that the Sheffield samples have significantly larger spin-flip cross-sections than their Budapest counterparts. The Sheffield samples clearly have both a larger non-correlated $\langle\mu^2_\perp\rangle^{1/2}$ and, to a less marked degree, a larger correlated $\langle\mu^2_\perp\rangle^{1/2}$. In addition, the gradient of the sloping background is steeper for the Sheffield samples than for the Budapest samples, confirming the conclusion that trace impurities of α-Fe induce non-correlated non-collinearity.

Perhaps the most important conclusion, however, is that the magnitudes of $\langle\mu^2_\perp\rangle^{1/2}$, while probably overestimated, imply that the *vast majority* of the magnetic moments in the samples are found in some form of non-collinear order. The magnitudes of $\langle\mu^2_\perp\rangle^{1/2}$ estimated from the cross-sections are the mean moment *per atom*. If only a small fraction of the atoms carry a non-collinear moment, the magnitudes of $\langle\mu^2_\perp\rangle^{1/2}$ would need to be scaled accordingly. This conclusion is consistent with the band theory calculations of Lorenz and Hafner [1], which suggest that the moments on the iron atoms in $Fe_{90}Zr_{10}$ have *on average* a non-collinear component of $\sim 2\ \mu_B$, making an angle of $\sim \cos^{-1}(1.3/2.35) = 56.4°$ to the mean ferromagnetic direction. The magnitudes of the non-collinear components in table 2 are comparable to these theoretical values, although they are large compared to an experimentally determined total moment per iron atom of $\sim 1.5\ \mu_B$, measured by Mössbauer spectroscopy [5].

Even so, although the analysis here can only put an upper limit on the moment, it strongly suggests that the fraction of the magnetic moments that are collinear with the mean ferromagnetic direction must be small. This conclusion potentially contradicts the qualitative model of Kaul *et al* [10, 11], who have proposed that the $Fe_{100-x}Zr_x$ metallic glasses have non-collinear magnetic clusters embedded in a ferromagnetic matrix. More likely is the cluster model of Kiss *et al* [12] who suggest that *all* the moments are found in non-collinear clusters, or some form of 'wandering axis' as proposed by Ryan *et al* [4]. Unfortunately, the band structure calculations of Lorenz and Hafner [1] do not extend to a discussion of spatially correlated non-collinear ferromagnetism. In the light of the agreement between the theory and the experimental results presented here, it would be useful to make such an extension for further comparison.

Further distinction between cluster and 'wandering axis' models could result from the presentation in absolute scattering units of previously published small-angle neutron scattering measurements [14], and will be the subject of future experiments to smaller Q on D7.

5. Conclusions

The presented spin-flip cross-sections and discussion have two important conclusions. Firstly, the establishment of correlated non-collinear ferromagnetism, while not allowing an unambiguous determination of the magnetic structure, permits some distinction between

previously proposed models. Only a model that allows for a vast majority of the magnetic moments in the systems to be significantly non-collinear can explain the magnitudes of the observed cross-sections. The energy window of the measurements also dictates that the non-collinear structure must also be the mean magnetic structure of the system. Secondly, the dependence of the magnetic structure on trace impurities of α-Fe in the Sheffield samples, something that was not immediately obvious from standard measurement techniques, has important ramifications for any previously presented data.

Acknowledgments

The authors would like to thank Mr J Newell of the University of Sheffield for his aid in the fabrication of samples, and the ISIS facility for the use of the LAD diffractometer. The financial support of the Hungarian Scientific Research Fund (OTKA T-038383) is very gratefully acknowledged.

Appendix. On the absolute calibration of the cross-sections and the accuracy of the data

The polarized neutron data have been carefully analysed and calibrated for presentation on an absolute scale. The raw data were corrected for background, absorption, resolution, instrument inefficiency and multiple scattering. On IN20, the background was measured using indium foil of approximately the same attenuation as the samples wrapped around empty sample frames. On D7, two measurements were taken to account for the background: one with no sample in a sample frame; and one with neutron absorbing cadmium. For both instruments the resulting measurements were matched to the attenuation of the respective samples. The incoherent scattering from vanadium plates was used as a calibration standard on both instruments. Measurements of the background and the vanadium for each flipper state were taken over the same Q-range as the data. After normalizing to monitor, the background could be directly subtracted from the raw data. The absorption cross-sections were calculated from the tabulated cross-sections [25] and the data corrected for absorption by integrating the path length through the sample. The vanadium data were then normalized to unity. Dividing the data by the corresponding normalized vanadium corrected for detector efficiency, Q-resolution and instrument geometry. The corrections of Wildes [31] were applied to adjust for imperfect polarization. Instrument polarization inefficiencies were estimated by measuring the flipping ratios from a silicon (111) reflection on IN20, and from a quartz rod on D7. Silicon and quartz give, to a good approximation, only non-spin-flip scattering. Multiple scattering in both the vanadium and the sample was accounted for using the corrections of Sears [32] and Harders *et al* [33].

The resulting data for both the $Fe_{100-x}Zr_x$ metallic glasses and the vanadium were taken to be the single-scattering events. The vanadium data were scaled to its incoherent cross-section, $5.08/4\pi = 0.404$ b sr^{-1}/atom [25]. After scaling the number of atoms in the $Fe_{100-x}Zr_x$ samples relative to the number of atoms in the vanadium, the two data sets could be directly compared and the cross-sections put on an absolute scale.

Many factors show that the resulting cross-sections have been correctly derived. There is excellent agreement between the results collected on D7 and on IN20. On IN20, the total cross-sections in the limit ($Q \to \infty$) for all the samples at all temperatures agreed well with the expected $(1/4\pi)(((1-\frac{x}{100})b_{\mathrm{Fe}}+\frac{x}{100}b_{\mathrm{Zr}})^2+\frac{x}{100}(1-\frac{x}{100})(b_{\mathrm{Fe}}-b_{\mathrm{Zr}})^2+\sigma_{inc})$ b sr^{-1}/atom. Data were taken for the same samples at different times and under different sample environment conditions. Separate background, vanadium and polarization correction measurements accompanied each measurement. The calculated cross-sections after calibration were in close agreement, confirming that there was no random error in any of the measurements.

Further checks as to the validity of the magnitude of a magnetic cross-section may sometimes be carried out with the aid of bulk susceptibility measurements. In the quasielastic scattering limit, the Kramers–Krönig relationship may be used to determine a magnetic cross-section at $Q = 0$ Å^{-1} from the magnetic susceptibility [34]. Likewise, the integration of the magnetic cross-section over an approximation of a Brillouin zone should correlate with the square of the magnetic moment [35]. While these methods work well for paramagnets and spin glasses where the total magnetic cross-section can be isolated with the aid of neutron polarization analysis, unfortunately the same cannot be said for non-collinear ferromagnets. The spin-flip data shown in figures 2 and 3 may be directly related to the *non-collinear* magnetic susceptibility using these techniques, but not directly to either the *collinear* or the *total* susceptibility. The equipment necessary to measure the non-collinear susceptibility of these samples in a field of 20 kOe was not available to the authors at the time of writing. The analysis and discussion in section 4.2 therefore represent the current limit of further checks.

The presence of peaks in the spin-flip cross-sections might be attributable to poor correction of the polarization inefficiencies. This is considered highly unlikely in the light of the agreement between the D7 and the IN20 data, even though the quality of the polarization differed considerably between the two instruments. In addition, if non-spin-flip scattering were considered in the derivation of the spin-flip cross-sections, the resultant peaks would be of the same width in non-spin-flip and spin-flip cross-sections at all temperatures. This is certainly not true for $T > T_C$, confirming that the polarization corrections have been correctly applied and that the spin-flip cross-sections have peaks.

Similarly, the presence of non-collinear ferromagnetic clusters, either from α-Fe or from glassy $Fe_{92}Zr_8$, could result in a depolarization of the neutron beam by the sample itself. Analysis of data from small-angle neutron scattering suggests that there may be clusters with correlation lengths of between 20 and 1500 Å [14]; however, it is impossible to determine whether the components of magnetic moments that contribute to these clusters are collinear or non-collinear. The sample depolarization is not expected to be a significant factor. Previous experience proves that ferromagnetic nanoparticles do not significantly depolarize a neutron beam (e.g. [36]). In addition, transmission measurements through the samples also showed no variation of the flipping ratio with temperature. As significant peaks were not observed for $T > T_C$, the measured spin-flip cross-sections are believed to be representative of the samples. Finally, neutron depolarization by the sample is well known to depend strongly on the neutron wavelength (e.g. [15]). The wavelength for the measurements on IN20 ($\lambda \sim 1.5$ Å) differed from the wavelength for the D7 measurements ($\lambda \sim 3.1$ Å) by almost a factor of two, yet the same cross-sections were observed from the two measurements. Given the large difference in wavelength between the two measurements, the fact that the measurements correspond so closely between the two instruments presents strong evidence that the sample is not randomly depolarizing the beam.

References

[1] Lorentz R and Hafner J 1995 *J. Magn. Magn. Mater.* **139** 209
[2] Kakehashi Y and Tanka H 1995 *The Magnetism of Amorphous Metals and Alloys* ed J A Fernández-Baca and W-Y Ching (Singapore: World Scientific)
[3] Kaptás D, Kemény T, Kiss L F, Gránásy L, Balogh J and Vincze I 1993 *J. Non-Cryst. Solids* **156–158** 336
[4] Ryan D H, Coey J M D, Batalla E, Altounian Z and Ström-Olsen J O 1987 *Phys. Rev.* B **35** 8630
[5] Ren H and Ryan D H 1995 *Phys. Rev.* B **51** 15885
[6] Ryan D H, van Lierop J, Pumarol M E, Roseman M and Cadogan J M 2001 *J. Appl. Phys.* **89** 7039
[7] Read D A, Moyo T and Hallam G C 1984 *J. Magn. Magn. Mater.* **44** 279
[8] Saito N, Hiroyoshi H, Fukamichi K and Nakagawa Y 1986 *J. Phys. F: Met. Phys.* **16** 911

[9] Vincze I, Kaptás D, Kemény T, Kiss L F and Balogh J 1994 *Phys. Rev. Lett.* **73** 496
[10] Kaul S N 1988 *J. Phys. F: Met. Phys.* **18** 2089
[11] Babu P D and Kaul S N 1997 *J. Phys.: Condens. Matter* **9** 7189
[12] Kiss L F, Kemény T, Vincze I and Gránásy L 1994 *J. Magn. Magn. Mater.* **135** 161
[13] Rhyne J J, Erwin R W, Fernández-Baca J A and Fish G E 1988 *J. Appl. Phys.* **63** 4080
[14] Fernández-Barquín L, Gómez Sal J C, Kaul S N, Barandiarán J M, Gorría P, Pedersen J S and Heenan R 1996 *J. Appl. Phys.* **79** 5146
[15] Ryan D H, Cadogan J M and Kennedy S J 1996 *J. Appl. Phys.* **79** 6161
[16] Ryan D H, Cadogan J M and van Lierop J 2000 *Phys. Rev.* B **61** 6816
[17] Karlsson L, McGreevy R L and Wicks J D 1999 *J. Phys.: Condens. Matter* **11** 9249
[18] Moon R M, Riste T and Koehler W C 1969 *Phys. Rev.* **181** 920
[19] Cowley R A, Patterson C, Cowlam N, Ivison P K, Martinez J and Cussen L D 1991 *J. Phys.: Condens. Matter* **3** 9521
[20] Wildes A R, Cowley R A, Al-Heniti S, Cowlam N, Kulda J and Lelièvre-Berna E 1998 *J. Phys.: Condens. Matter* **10** 2617
[21] Wildes A R, Cowlam N, Al-Heniti S, Kiss L F and Kemény T 2000 *Physica* B **276–278** 712
[22] Wildes A R, Cowlam N, Al-Heniti S, Kiss L F and Kemény T 2001 *J. Magn. Magn. Mater.* **226–230** 1470
[23] Al-Heniti S 1999 *PhD Thesis* University of Sheffield
[24] Hannon A C, Howells W S and Soper A K 1990 *Inst. Phys. Conf. Ser.* **107** 193
[25] Sears V F 1992 *Neutron News* **3** 26
[26] Brown P J 1995 *International Tables for Crystallography* vol C, ed A J C Wilson (Dordrecht: Kluwer) pp 391–9
[27] Acet M, Roessel T, Wassermann E F, Andersen K H, Kulda J, Murani A P and Wildes A 2000 *J. Phys. Soc. Japan Suppl.* A **69** 108
[28] Howells W S and Hannon A C 1999 *J. Phys.: Condens. Matter* **11** 9127
[29] Blétry J and Sadoc J F 1975 *J. Phys. F: Met. Phys.* **5** L111
[30] Guoan W, Cowlam N, Davies H A, Cowley R A, Paul D McK and Stirling W 1982 *J. Physique Coll.* **13** C7 71
[31] Wildes A R 1999 *Rev. Sci. Instrum.* **70** 4241
[32] Sears V F 1975 *Adv. Phys.* **24** 1
[33] Harders T M, Hicks T J and Wells P 1985 *J. Appl. Crystallogr.* **18** 131
[34] Hicks T J 1995 *Magnetism in Disorder* (Oxford: Clarendon) p 9
[35] Rainford B D, Dakin S J and Cywinski R 1992 *J. Magn. Magn. Mater.* **104–107** 1257
[36] Casalta H, Schleger P, Bellouard C, Hennion M, Mirebeau I, Ehlers G, Farago B, Dormann J-L, Kelsch M, Linde M and Phillipp F 1999 *Phys. Rev. Lett.* **82** 1301